

ASCE-SP#23 SM#135

CLASS A PREDICTION OF DRIVEN PILE BEHAVIOR

R.G. Campanella<sup>1</sup>, M.ASCE, A. Sy<sup>2</sup>, M.ASCE, M.P. Davies<sup>3</sup> and  
P.K. Robertson<sup>4</sup>, M.ASCE

ABSTRACT: The axial loading behaviour of two driven piles is predicted as part of the pile capacity prediction event that will be held in conjunction with the 1989 ASCE Foundation Engineering Congress. The analyses were carried out using procedures in current engineering practice and based on the in-situ and laboratory test data provided. The authors have no prior knowledge of the local geological conditions or results of the load tests conducted to date.

INTRODUCTION

Northwestern University (NWU) will be conducting a series of pile load tests to evaluate the capacity and load transfer characteristics of four piles in conjunction with the 1989 ASCE Foundation Engineering Congress. The test site is located on the Lakefill in the Evanston Campus of Northwestern University. Geotechnical engineers have been invited to make predictions of capacity and load transfer behavior of the piles before the results are published.

The objective of the pile prediction event is "to permit a state of the practice review of the profession's ability to predict single pile response under axial loading." To this end, Northwestern University has requested predictions of the behavior of four different types of piles with respect to: capacity at 2 weeks, 1 month and 1 year after pile installation; lower bound estimate of capacity with 90% confidence that the actual value will be higher; load-pile butt settlement; axial load distribution along the piles

- 
- 1 - Professor, Dept. of Civil Eng., Univ. of British Columbia, 2324 Main Mall, Vancouver, B.C., Canada, V6T 1W5.
  - 2 - Graduate Student, Dept. of Civil Eng., Univ. of British Columbia, 2324 Main Mall, Vancouver, B.C., Canada, V6T 1W5.
  - 3 - Engineer, Klohn Leonoff Ltd., 10180 Shellbridge Way, Richmond, B.C., Canada, V6X 2W7.
  - 4 - Professor, Dept. of Civil Eng., Univ. of Alberta, Edmonton, Alberta, Canada, T6G 2G7 (formerly at Univ. of British Columbia).

at failure and 50% of the failure loads; residual stress distributions and pore water pressure generation and dissipation.

This paper is in response to Northwestern University's request but is restricted to prediction of the behaviour of the two driven piles: a close-ended pipe pile and a steel H-pile. To meet the objective of this event, the study consisted of a review and assessment of the soils and pile data provided, estimation of pile capacities, load-pile top settlement, axial load distributions along the pile length, pore pressure generation and dissipation, and a discussion and assessment of the predictions.

#### SITE CONDITIONS

The stratigraphy at the test site consists of 23 ft of fine clean sand (SP), 35 ft of firm clay (CL), 12 ft of stiff clay (CL) and 10 ft of hard silt (ML) overlying bedrock at a depth of 80 ft. The groundwater table was 10 ft below grade at the time of the site investigation but was at a depth of 15 ft, the same level as that of adjacent Lake Michigan, just prior to pile installation in May 1988.

The field information provided by NWU consists of data from electric cone penetration tests (CPT), standard penetration tests (SPT), Menard pressuremeter tests (PMT), flat dilatometer tests (DMT), field vane shear tests (FVT), and rotary drill holes with sampling. The laboratory test data consist of moisture contents, grain size distributions of sand samples, oedometer tests, unconsolidated-undrained (UU) triaxial compression tests, direct shear tests and  $K_0$ -consolidated, undrained ( $CK_0U$ ) triaxial compression and extension tests of clay samples.

Because the test piles are 50 ft long, only the surface sand layer and the underlying firm clay stratum are of interest. The sand is a fill that was placed in 1966. It is fine grained, with an average mean grain size of 0.25 mm with less than 5% passing the No. 200 mesh sieve. The clay has low plasticity (P.I. of 18%) with an average water content of 23%, slightly above the plastic limit of 20%. NWU reported that the piezometric readings in the clay suggested hydrostatic conditions prior to pile installation.

The pertinent field and laboratory test data are reviewed and interpreted as discussed below.

#### FIELD DATA

CPT. The CPT data consist of four electric friction cone tests (CPT1 to CPT4) conducted with a standard 10 cm<sup>2</sup> cone (ASTM D3441-86), and one electric piezometer cone test (CPTU) performed with a 15 cm<sup>2</sup> cone and with a pore pressure sensing element located mid-height on the conical tip. The test data indicate that the sand deposit is variable in density and its thickness increases to the south. The trend in the cone resistance profiles, however, identifies three zones in the sand deposit: a dense upper zone overlying a medium dense zone near the water level which overlies a denser zone again above the clay stratum. In the clay, the CPT data suggest a relatively consistent deposit with low cone tip and low friction sleeve resistances.

The closest CPT to the test section is CPT1 which is 15 to 25 ft from the driven test pile locations. Based on CPT1, the average tip resistance ( $q_c$ ) and friction sleeve resistance ( $f_s$ ) values are summarized in Table 1. Also shown in Table 1 are the friction angles ( $\phi'$ ) evaluated from  $q_c$  in the sand as suggested by Robertson and Campanella (1983).

Table 1. CPT1 Average Tip and Friction Sleeve Resistances

Depth (ft)	$q_c$ (tsf)	$f_s$ (tsf)	$\phi'$ (degree)
0 to 10	150.0	1.4	>45
10 to 15	90.0	0.9	40
15 to 23	220.0	1.6	45
23 to 50	10.0	0.15	-

Although the values given in Table 1 represent approximate averages for sounding CPT1, a sensitivity analysis showed that they provided similar predictions of pile capacity as the measured values taken every 0.25 ft.

The pore pressure dissipation data from CPTU indicate a horizontal coefficient of consolidation ( $c_h$ ) in the overconsolidated region of about  $5.5 \times 10^{-3}$  cm<sup>2</sup>/s.

SPT. The SPT's were performed in the sand deposit in two drill holes using two different hammer systems: a safety hammer in Test Hole B-1 and an automatic hammer in Test Hole PM-1. Borehole procedures, dimensions of the split spoon, whether a liner was used, procedures used in the rope and cathead method, tripping mechanism in the automatic system, and hammer energy efficiencies were not given. The SPT data, however, do confirm the three zones of different densities in the sand deposit. Ratios of the automatic hammer blow counts to the corresponding safety hammer blow counts at the same depth vary from 0.33 to 0.51. This would suggest that if the automatic hammer was delivering 100% of the theoretical maximum SPT energy (4200 in lb), the safety hammer would only be delivering an average energy ratio of about 40%. Table 2 summarizes the average N values (blows/ft) in the sand deposit, together with equivalent N values derived from the CPT data using the  $q_c/N$  versus  $D_{50}$  relationship proposed by Robertson et al. (1983).

Table 2. Average N Values in Sand Deposit

Depth (ft)	Safety Hammer	Automatic Hammer	Inferred from CPT ( $q_c/N=5$ )
0 to 10	55	25	30
10 to 15	30	10	18
15 to 23	60	26	44

If the equivalent N values derived from the CPT are assumed to represent N values at an energy ratio of about 60%, the average derived energy ratios of the safety hammer and automatic trip hammer are 38% and 94%, respectively. These derived energy ratios are quite possible when compared to global energy ratios reported in the literature.

PMT. Five Menard PMT's were conducted in test Hole PM-1; 2 in sand and 3 in clay. The expansion tests were done in a prebored hole, except for 2 tests in clay in which the instrument was pushed into the bottom of the drill hole without predrilling. There were insufficient data provided to evaluate the effect of the different procedures in the clay. There were also no detailed PMT data presented in the NWU report, except one pressure expansion curve and tabulations of test values and parameters as interpreted by Woodward Clyde Consultants. The report indicates a friction angle ( $\phi$ ) of  $37^\circ$  in the sand, undrained shear strengths ( $S_u$ ) of 0.36 to 0.43 tsf in the clay, and unload-reload Young's moduli of 1165 tsf in the sand and 40 to 70 tsf in the clay.

DMT. The DMT's were conducted in two holes in the depth range of 18 to 49 ft. The interpreted results in the NWU report indicate dilatometer moduli,  $E_d$ , of about 1300 bars in the sand and 20 bars in the clay.

FVT. The FVT data in the range of interest indicate  $S_u$  of 660 to 820 psf, and an average sensitivity of 2.0. The test data suggest a decreasing trend in the ratio of  $S_u$  to effective overburden pressure ( $S_u/p'$ ) with an average value of 0.25. The type of equipment and test procedures used for the FVT, however, were not reported.

#### LABORATORY DATA

The oedometer test data indicate that the firm clay stratum is slightly overconsolidated (O.C.) to normally consolidated (N.C.) under the present overburden pressure. Based on the oedometer results, the vertical coefficient of consolidation,  $c_v$ , values are  $5 \times 10^{-4}$  cm<sup>2</sup>/s in the N.C. region and  $2 \times 10^{-3}$  cm<sup>2</sup>/s in the O.C. region. Assuming a  $c_h/c_v$  ratio of 2 to 4 applicable to most clays yields an estimated  $c_h$  of 4 to  $8 \times 10^{-3}$  cm<sup>2</sup>/s for the O.C. region. Note that these oedometer inferred  $c_h$  values are similar to those derived from the CPTU.

The UU triaxial compression test data show  $S_u$  ranging from 500 to 840 psf with an average of 600 psf and  $S_u/p'$  ratios from 0.37 to 0.17, generally decreasing with depth, with an average of 0.23.

The direct shear tests under drained conditions for the clay sample at 40 ft depth indicate an effective friction angle of  $23^\circ$ .

The CK<sub>0</sub>U triaxial compression test data indicate an initial undrained Young's modulus of 4200 kpa and a pore pressure parameter at failure,  $A_f$ , of about 0.3.

#### PILE DATA

The two driven test piles, 18 in O.D. by 0.375 in wall thickness pipe and HP 14 x 73, were driven with a Vulcan 06 single acting steam hammer to final resistances of 10 and 12 blows/ft,

respectively, at approximately 50 ft depth. The hammer has a manufacturer's rated energy of 19,500 ft lb. No dynamic pile monitoring was indicated in the NWU report to measure hammer energy transfer. The pipe pile was closed with a 19 in diameter end plate which represents 0.5 in projection from the pile wall. Prior to installation of the close-ended pipe pile, a 12 in diameter hole was augered to a depth of 23 ft at the pile location. The volume of soil removed (out of hole) during preaugering was not reported. There was also no report on the depth or amount of gapping around the driven piles after installation.

Both piles were instrumented along their length with vibrating wire strain gauges and tell-tale rods.

#### LOAD TEST PROCEDURE

The load tests will be performed in accordance with the Standard Loading Procedure described in ASTM D1143-81. The test loads will be applied to the pile using a hydraulic jack placed against an anchored reaction frame. The piles will be tested to "failure," however, the failure criterion was not specified. Although a plunging type of failure is anticipated because the lower part of the pile is embedded in clay, the interpreted failure load from the test will likely represent a range of values.

#### LIMITATIONS OF TEST DATA

The pile analyses and prediction in this study are based on the field and laboratory test data provided and the author's collective experience. The detailed geology of the site and mineralogy of the soil deposits are not known. The CPT's provided the only data concerning the variability of the soil deposits across the test site. However, only CPT1 was within 40 ft of the test piles. A comparison of the CPT data indicates that CPT1 gives generally higher tip resistance values. Because of its location, CPT1 was assumed to be representative of the conditions at the pile locations. In practice, one would likely use the lower, or more conservative, values from the other CPT's for design.

The CPTU dissipation tests were conducted with the piezometer element on the face of the cone. The authors consider that it would have been more appropriate to use a cone with the filter element located behind the tip, as this location would better represent the pore pressure generation and dissipation characteristics around the shaft of a driven pile.

The effect of pre-augering at the pipe pile location represents a major uncertainty in terms of predicting the pipe pile capacity. There is as yet no reliable or practical way of quantifying this effect. The effect on the pile capacity and load deformation behaviour is highly dependent on the actual construction procedure. Another factor hard to quantify is the stress reduction along the pile length caused by the oversized shoe on the pipe pile.

The effect of the installation of adjacent piles on the driven piles is another uncertainty. The test plot is 20 ft by 35 ft and altogether contains 13 piles, typically 8 to 9 ft apart. Although

the anchor H-piles are often considered "non-displacement" piles, compaction of the sand deposit and excess pore pressure generation in the underlying clay deposit could occur. The densification effect might partially compensate for the loosening effect of the pre-augering and oversized shoe, while the latter effect might affect the pore pressures recorded in Piezometers P1 and P2 located near the pipe pile.

The limitations and uncertainties described above will undoubtedly affect the reliability and accuracy of the predictive methods, whether they be empirical or theoretical. Several methods of analyses were carried out as described below, using procedures in current engineering practice. From the range of results obtained, judgement based on qualitative considerations of the above factors, was used to select the "most likely" values for the prediction.

#### ANALYSES

Pile Capacities. Both static and dynamic methods of analysis were performed to predict the capacity of the driven piles. The static prediction methods investigated, references and type of data used in the analysis are summarized in Table 3.

Table 3. Static Prediction Methods

Method	Reference	Data Used
Schmertmann	Schmertmann (1978)	CPT $q_c$ & $f_s$
LCPC	Bustamante and Gianceselli (1982)	CPT $q_c$
de Ruiter & Beringen	de Ruiter and Beringen (1979)	CPT $q_c$ & $f_s$
API	American Petroleum Inst. (1987)	Field $\phi$ & Lab $S_u$
Dennis & Olson	Dennis & Olson (1983a & b)	Field $\phi$ & Lab $S_u$

Table 4 shows the computed ultimate (long term) capacities by the different methods for the two driven test piles. For the CPT based methods, the  $q_c$  and  $f_s$  values in Table 1 were used. For the other methods, the soil parameters assumed were: pile/sand interface friction angles of 35° for the top and bottom zones and 30° for the middle sand zone, and  $S_u$  of 600 psf based on laboratory UU test. The effective unit weights assumed were 105 pcf for the sand above water table (10 ft depth), 52.6 pcf for submerged sand and 60.0 pcf for submerged clay. For the H-pile, an enclosing square (14 in side width) was assumed for the pile/soil friction calculation and only the cross-sectional area of the steel was used for end bearing calculation. The effects of pre-augering and oversized shoe were not considered in the capacity calculations shown in Table 4 for the pipe pile.

Two dynamic methods were also investigated. It is recognized that dynamic methods, at best, are more appropriate in sands than in clays for estimating static pile capacities. The simple Engineering News Formula (Peck et al. 1974) indicates ultimate capacities (assumed factor of safety of 6) of 90 and 106 tons for the pipe pile

Table 4. Calculated Ultimate Capacities by Static Methods

Method	Friction Sand (tons)	Friction Clay (tons)	Tip Clay (tons)	Total Capacity (tons)
<b>18 INCH PIPE PILE</b>				
Schmertmann	88.6	20.4	17.7	126.7
LCPC	87.3	19.1	8.8	115.2
de Ruiter & Beringen	58.2	47.7	8.0	113.9
API	36.8	38.2	4.8	79.8
Dennis & Olson	50.1	38.2	4.8	93.1
<b>HP 14 X 73</b>				
Schmertmann	79.4	20.2	1.5	101.1
LCPC	86.6	18.9	0.8	106.3
de Ruiter & Beringen	57.7	47.3	0.7	105.7
API	29.4	37.8	0.4	67.6
Dennis & Olson	39.8	37.8	0.4	78.0

and H-pile, respectively. For both pile types, wave equation analysis using the GRLWEAP (Goble et al., 1988) program suggests capacities of only about 50 tons. This value could be considered as a lower limit, since set-up in the clay deposit was not considered in the wave equation approach using the final blow count at the end of initial continuous driving.

Table 4 indicates that, in general, the friction resistance in the sand can be expected to provide between 50% and 80% of the predicted failure capacities. The CPT based methods predict higher frictional capacities in the sand than those by the API or Dennis and Olson methods. However, the pre-augered 12 in. diameter hole and the oversized shoe could significantly reduce the friction resistance for the pipe pile. Hence, the prediction of the pipe pile capacity is uncertain.

Table 4 also indicates that the frictional capacities of both the pipe pile and H-pile are very similar. The predicted tip resistance of the H-pile is significantly smaller than that of the pipe pile because of the smaller assumed cross-sectional area of the steel.

Since the CPT based methods have generally provided reliable estimates of pile capacity (Robertson et al., 1988; Briaud and Tucker, 1988), the authors have put greater reliance on them. The LCPC method has the advantage that it requires only the CPT  $q_c$  values and incorporates different pile installation methods, although no allowance has been directly included to account for the effects of pre-augering and an oversized shoe. Based on a consideration of the method of pile installation, the predicted capacities for the driven piles are given in Table 5. The formulas used in the LCPC method are summarized in Table 6.

Lower Bound Capacities. A lower bound capacity, with 90% confidence that the actual value will be higher than this lower bound, was estimated using the second-moment reliability index approach (Hasofer and Lind, 1974). The computer program RELAN

Table 5. Predicted Ultimate Capacities

	Friction Sand (tons)	Friction Clay (tons)	Tip Clay (tons)	Total Capacity (tons)	Lower Bound Capacity (tons)
18 inch pipe	65	20	8	93	62
HP 14 x 74	80	20	1	101	65

Table 6. Formulas Used in LCPC Method

Unit Shaft Resistance, f	Unit End Bearing, $q_p$
$f = \sum \frac{q_c}{\alpha}$	$q_p = q_c K_c$

where

- $q_c$  = CPT tip resistance (see Table 1)
- $\alpha$  = empirical skin friction coefficient
  - = 200 for sand
  - = 30 for clay\*
- $K_c$  = empirical bearing capacity factor
  - = 0.5 for clay

\*Limit f value of 0.15 tsf was used for clay

(Foschi, 1988), which incorporates the generalized Rackwitz-Fiessler algorithm, was used to compute the probability of a load exceeding the predicted capacity. Uncertainties of the parameters in the LCPC method were included in the analysis by defining the following as random variables: CPT tip resistance ( $q_c$ ), empirical skin friction coefficient ( $\alpha$ ), empirical bearing capacity factor ( $K_c$ ), and an error term associated with the uncertainty of the prediction method. The random variables were assumed to be normally distributed with mean values as those used in the prediction and coefficients of variation between 0.2 and 0.3. Figure 1 shows the results of the analysis in the form of a cumulative density function, which gives the probability that the capacity will have a value less than or equal to any selected value. Based on this analysis, a lower bound estimate of capacity with 90% chance of values being higher, is about 62 tons for the 18 in pipe pile and 65 tons for the H pile. These values are also indicated in Table 5.

Load-Pile Top Settlement. The load transfer method of estimating pile settlement as incorporated in the program PILSET (Olson, 1985) was used to predict the pile top settlement behavior and axial load distributions along the length of the pipe pile. In this method, the pile is idealized as a series of discrete elements (elastic springs) and the adjoining soil is represented by non-linear springs on fixed supports. Several methods have been proposed to estimate

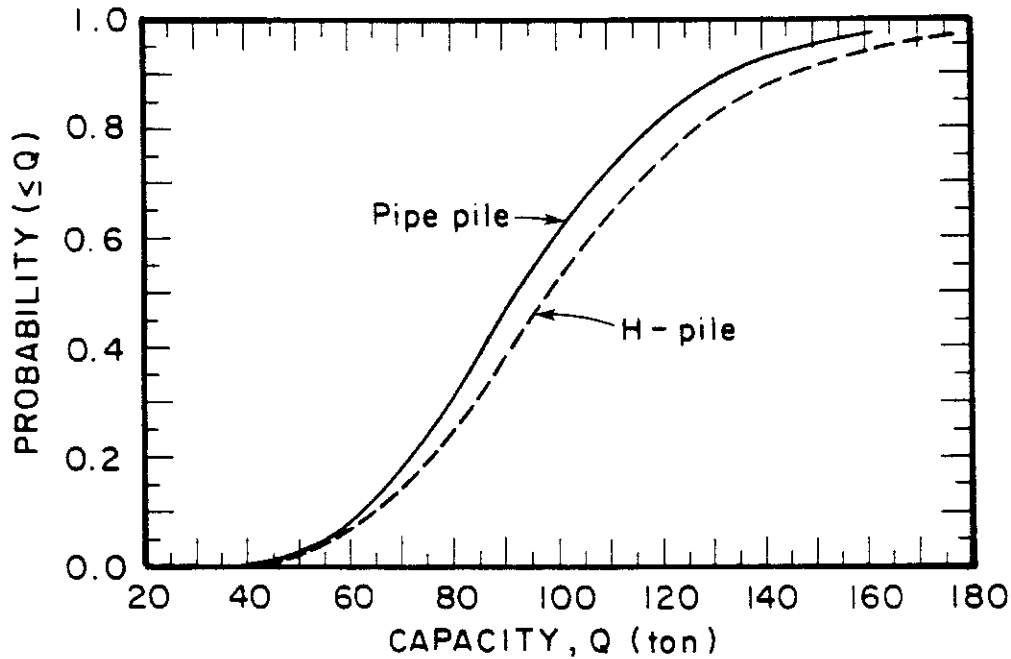


Figure 1. Cumulative Density Functions for Predicted Pile Capacities

the load-deformation curves for the soil springs. The different load transfer curves investigated for this prediction are summarized in Table 7. The limiting unit shaft and tip resistance values back-calculated based on the predicted capacities given in Table 5, were used to define the failure loads.

Table 7. Load Transfer Curves Investigated

Method	Reference	Comments
Coyle	Coyle & Reese (1966); Coyle & Sulaiman (1967)	For clay; for sand
Vijayvergiya	Vijayvergiya (1977)	
Hyperbolic	Kraft et al. (1981)	PMT unload-reload moduli
Bilinear	Aschenbrenner & Olson (1984)	Sett. at failure = 0.1 in

Figure 2 shows the results of the analysis for the pipe pile. Note the wide variation in the predicted load-settlement curves.

Based on the assumption that over 90% of the capacity is derived from shaft friction, it is reasonable to assume that, before failure, the pile top will settle less than the theoretical elastic compression for an unsupported pile. The elastic compression line has been included in Figure 2 as a reference. Hence, the authors predict that, for the pipe pile, the pile top-load settlement curve should approximate the curve represented by the bilinear method.

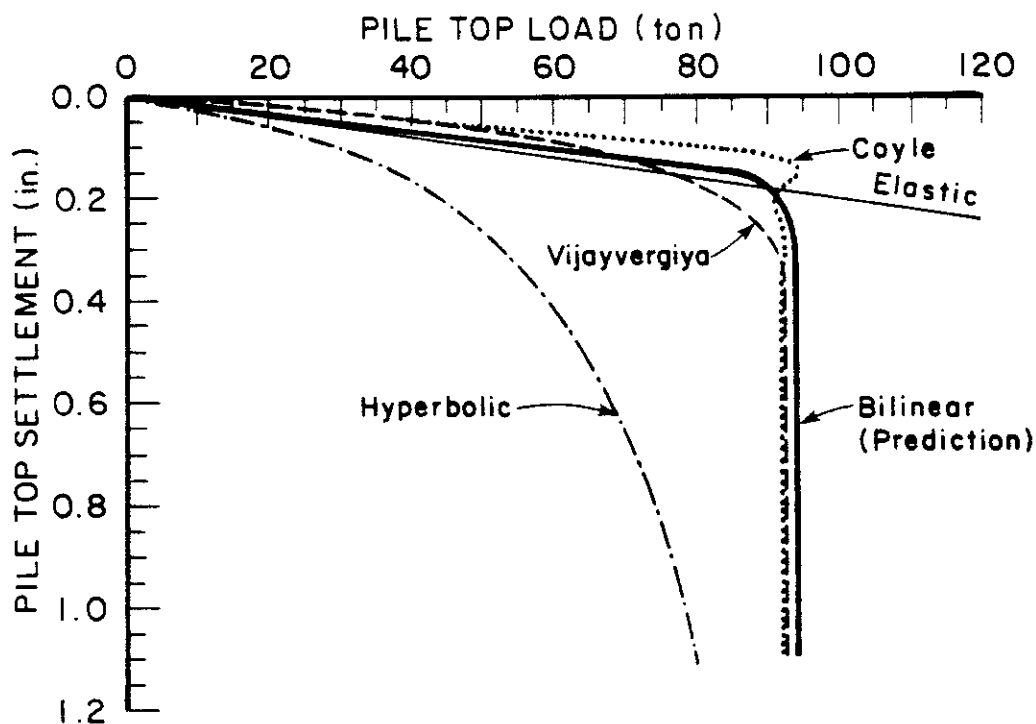


Figure 2. Predicted Load-Pile Top Settlement for Pipe Pile

The predicted settlement at 50% of the failure load is about 0.07 in.

The H-pile could be expected to have a very similar pile top-load settlement curve except that slightly larger settlements would be expected close to failure. The soil plugged in the H-pile flanges would be expected to initially move with the pile except when the pile is close to failure, when the steel section should plunge into the soil below.

Axial Load Distributions. Based on the bilinear load transfer curves, the axial load distributions along the pipe pile length at the predicted failure load and at 50% of the failure load are shown on Figure 3.

Pore Pressures. Two pneumatic piezometers, P1 and P2, were installed at 35 and 48 ft depths, respectively, at locations approximately 5 ft from the pipe pile centreline. This distance represents a distance to pile radius ratio of about 6.7.

The cone penetration represents a model of the pipe pile installation. Hence, the pore pressures recorded on the face of the cone during penetration should represent the expected maximum pore pressures immediately beneath the base of the pipe pile during driving. Due to stress relief effects, the pore pressures along the shaft of the pipe pile could be expected to be between 60% and 80% of those at the base (i.e. between 60% and 80% of those recorded by the CPTU).

The radial extent that pore pressures are generated around a penetrating pile depends on the assumed  $G/S_u$  ratio. Based on cavity

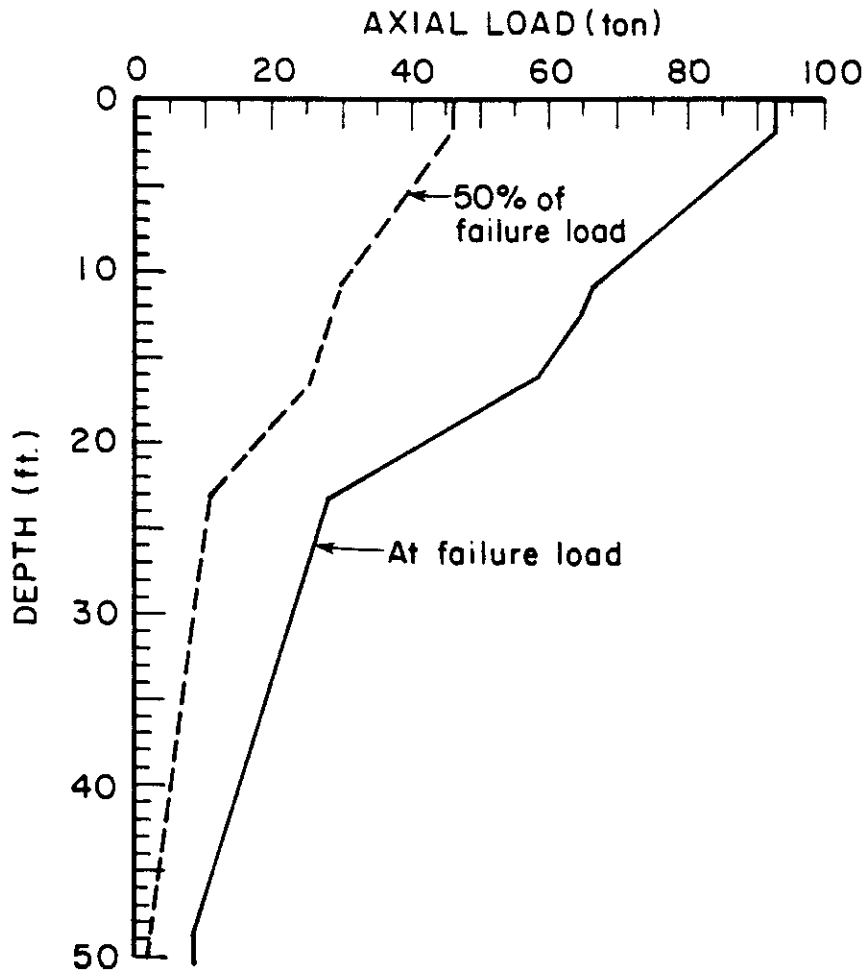


Figure 3. Predicted Axial Load Distribution for Pipe Pile

expansion theories and the measured CPTU data, a reasonable maximum distance to radius ratio of about 15 was assumed. Figure 4 presents a plot of pore pressure versus normalized radius showing the predicted maximum pore pressures during driving. Based on Figure 4, the maximum pore pressures recorded at piezometers P1 and P2 are 3800 psf and 5500 psf, respectively. These pore pressures can be expected to be generated as the base of the pipe pile passes the same elevation as the piezometers.

After the base of the pipe pile passes the elevation of each piezometer (P1 and P2), the pore pressures during driving could be expected to reduce to between 60% and 80% of these maximum values.

Clearly, there are considerable uncertainties or unknowns in the prediction of pore pressures adjacent to piles during driving. The pore pressures recorded at P1 and P2 could also be influenced by the driving of the nearby anchor H-piles. The recorded pore pressures could also be strongly influenced by the response time of the piezometers.

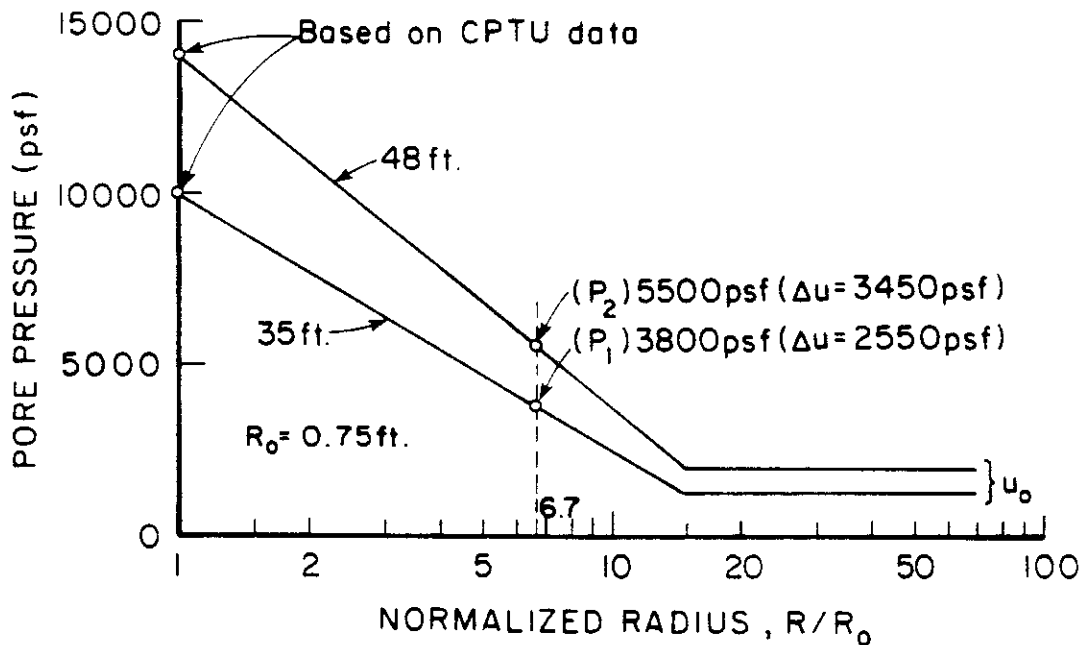


Figure 4. Predicted Maximum Pore Pressures During Pipe Pile Driving

The subsequent dissipation of excess pore pressures around a driven pile was estimated using the radial consolidation solutions as proposed by Randolph et al. (1979). The results of the analysis are shown in Figure 5 for excess pore pressure dissipations adjacent to the pipe pile wall. A range of  $G/S_u$  between 25 and 500 coupled with a range of  $C_h$  from  $4$  to  $8 \times 10^{-3} \text{ cm}^2/\text{s}$  was investigated. The  $CK_U$  triaxial compression test and PMT data indicate  $G/S_u$  between 15 and 60. A back analysis of the pore pressures measured on the cone tip during the CPTU, however, would suggest much higher  $G/S_u$  ratio. The authors believe that the curve represented by  $G/S_u = 100$  and  $C_h = 6 \times 10^{-3} \text{ cm}^2/\text{s}$  appears to provide a reasonable estimate of the excess pore pressure decay with time around the pile. The results suggest that 90% of the excess pore pressures would be dissipated about 7 weeks after pile driving and that full dissipation would occur after 1 year.

It has been shown that the increase in pile capacity with time after driving in clay has similar characteristics to the rate of dissipation of excess pore pressures. Thus, an estimate of the pile set-up with time can be obtained from a knowledge of the pore pressure dissipation. Based on the results in Figure 5, the predicted shaft and tip resistance components of the pipe pile in the clay at times 2 weeks, 1 month and 1 year after pile installation are summarized in Table 8. These increases in capacity, however, do not include the possible additional effect due to thixotropic regain of strength in the remoulded clay after pile driving.

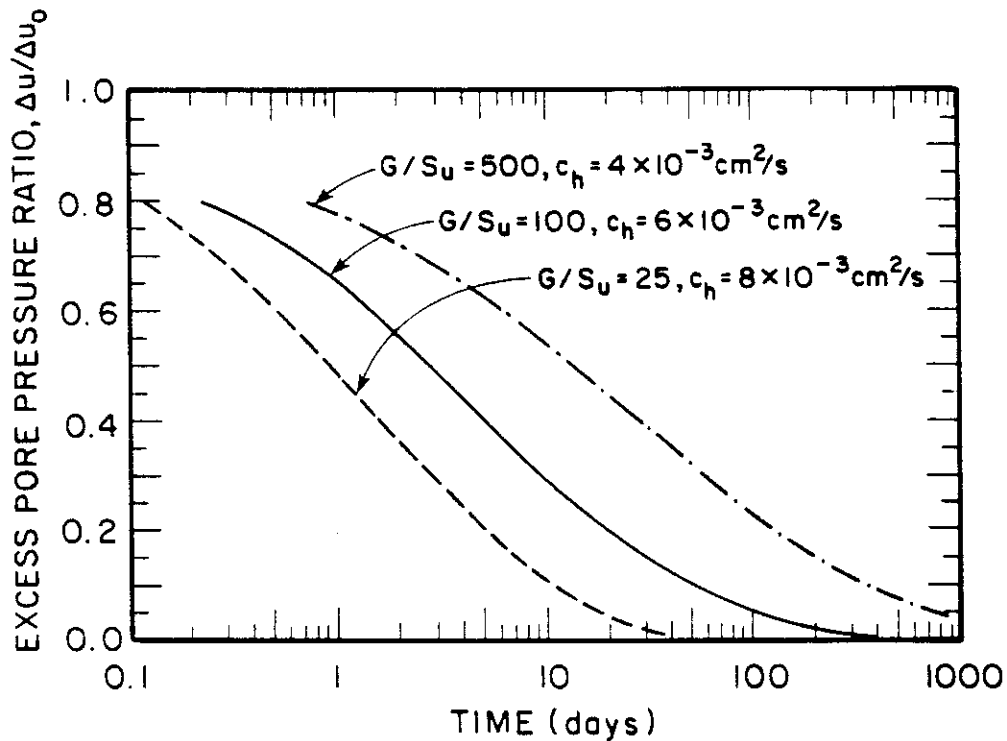


Figure 5. Predicted Pore Pressure Dissipation Around Pipe Pile

Table 8. Increase of Pipe Pile Capacity with Time

Time after Pile Installation	Amount of Excess Pore Pressure Dissipated (%)	Predicted Capacity in Clay (tons)
2 weeks	60 to 80	17 to 22
1 month	70 to 90	20 to 25
1 year	100	28

#### CONCLUSIONS

The axial loading behavior of two driven test piles at Northwestern University has been predicted using methods in current engineering practice. The limitations of the test data and the prediction methods investigated, and other uncertainties have been discussed. Because of the unknowns and uncertainties with regard to some aspects of pile installation, in-situ testing and test data interpretation, there is a large uncertainty in this pile prediction study.

#### ACKNOWLEDGEMENTS

The authors thank Professor R.O. Foschi for discussions on pile reliability analysis. The authors are also grateful to Ms. G. Breig for typing the manuscript and Mr. R. Brun for drafting the figures.

#### REFERENCES

1. American Petroleum Institute, Recommended Practice for Planning, Designing and Constructing Fixed Offshore Platforms, API RP 2A (17th Ed), 1987.
2. TB Aschenbrener & RE Olson, Prediction of Settlement of Single Piles in Clay, Symp. on Analysis and Design of Pile Foundations, ASCE, San Francisco, 1984, 41-58.
3. JL Briand & LM Tucker, Measured and Predicted Axial Response of 98 Piles, J.GED.(ASCE), 114(9), 1988, 984-1001.
4. M Bustamante & L Gianceselli, Pile Bearing Capacity Prediction by Means of Static Penetrometer CPT, Proc.ESOPT II, Amsterdam, 2, 1982, 493-500.
5. HM Coyle & LC Reese, Load Transfer for Axially Loaded Piles in Clay, J.SMFD(ASCE), 92(SM2), 1966, 1-26.
6. HM Coyle & IH Sulaiman, Skin Friction for Steel Piles in Sand, J.SMFD(ASCE), 93(SM6), 1967, 261-278.
7. J. de Ruiter & FL Beringen, Pile Foundations for Large North Sea Structures, Marine Geotechnology, 3(4), 1979, 267-314.
8. ND Dennis & RE Olson, Axial Capacity of Steel Pipe Piles in Clay, Geotechnical Practice in Offshore Engineering, ASCE, Austin, 1983a, 370-387.
9. ND Dennis and RE Olson, Axial Capacity of Steel Pipe Piles in Sand, Geotechnical Practice in Offshore Engineering, ASCE, Austin, 1983b, 389-402.
10. RO Foschi, RELAN (Reliability Analysis) Users Manual, Dept. of Civil Eng., Univ. of British Columbia, 1988.
11. Goble Rausche Likins and Associates, Inc., GRLWEAP Wave Equation Analysis of Pile Driving, 1988.
12. AM Hasofer and NC Lind, An Exact and Invariant First Order Reliability Format, J.EMD(ASCE), 1974, 111-121.
13. LM Kraft, RP Ray & T Kagawa, Theoretical t-z Curves, J.GED (ASCE), 107(GT11), 1981, 1543-1561.
14. RE Olson, PILSET Program User's Manual, Dept. of Civil Eng., The Univ. of Texas at Austin, 1985.
15. RB Peck, WE Hanson & T Thornburn, Foundation Engineering (2nd Ed), John Wiley and Sons, Inc., 1974.
16. HG Poulos & EH Davis, Pile Foundation Analysis and Design, John Wiley and Sons, Inc., 1980.
17. MF Randolph, JP Carter & CP Wroth, Driven Piles in Clay - The Effects of Installation and Subsequent Consolidation, Geotechnique, 29(4), 1979, 361-393.
18. PK Robertson & RG Campanella, Interpretation of Cone Penetration Tests - Part I (Sand), Canadian Geotech.J., 20(4), 1983.
19. PK Robertson, RG Campanella & A Wightman, SPT-CPT Correlations, J.GED(ASCE), 109(11), 1983, 1449-1459.

20. PK Robertson, RG Campanella, MP Davies & A Sy, Axial Capacity of Driven Piles in Deltaic Soils Using CPT, Proc.ISOPT 1, Orlando, Florida, 1988.
21. JH Schmertmann, Guidelines for Cone Penetration Test, Performance and Design, Fed. Highways Admin., Report FHWA-TS-78-209, Washington, 1978, 145 p.
22. VN Vijayvergiya, Load-Movement Characteristics of Piles, 4th Annual Symp. Ports'77(ASCE), Long Beach, 2, 1977, 269-284.

#### CONVERSION FACTORS

1 ft	=	0.3048 m
1 in	=	25.4 mm
1 ton	=	8.896 kN
1 psf	=	47.88 N/m <sup>2</sup>
1 tsf	=	95.76 kN/m <sup>2</sup>
1 bar	=	100 kN/m <sup>2</sup>
1 in lb	=	0.113 Joules
1 ft lb	=	1.356 Joules